

Space-variant polarization manipulation of a thermal emission by a SiO₂ subwavelength grating supporting surface phonon-polaritons

Nir Dahan, Avi Niv, Gabriel Biener, Vladimir Kleiner, and Erez Hasman^{a)}

Optical Engineering Laboratory, Faculty of Mechanical Engineering, Technion-Israel Institute of Technology, Haifa 32000, Israel

(Received 2 December 2004; accepted 22 March 2005; published online 2 May 2005)

Space-variant polarization manipulation of enhanced nondirectional thermal emission in a narrow spectral peak is presented. The emission is attributed to surface phonon-polariton excitation from space-variant subwavelength SiO₂ gratings. Polarization manipulation was obtained by discretely controlling the local orientation of the grating. We experimentally demonstrated thermal emission in an axially symmetric polarization distribution. Theoretical calculations based on rigorous coupled-wave analysis are presented along with experimental results. © 2005 American Institute of Physics. [DOI: 10.1063/1.1922084]

Thermal emission from absorbing material is considered to be incoherent and unpolarized, and accordingly is regarded as spontaneous emission. The surface properties of the absorbing material have a profound impact on the emission's optical properties, and can be manipulated to produce a partially coherent and partially polarized radiation emission.¹⁻⁶ Recently, it was shown that by etching a uniform grating on a SiC substrate, a highly directional peak of thermal emission was achieved.^{1,2} Furthermore, spectral resonance and nondirectional emission were observed at certain frequencies.² In these instances, a connection between the emission and the surface properties was established by studying the excitation of surface phonon-polaritons (SPPs). The underlying microscopic origin of the SPP is the mechanical vibration of the atoms. A surface polariton has a longer wave vector than the light waves propagating along the surface with the same frequency. For this reason, they are called "nonradiative" surface polaritons. By coupling the surface polaritons with the propagating wave by means of an additional prism or grating, one can produce either increased resonant absorption or directional emission. Because SPPs are able to be excited only by TM-polarized propagating waves, the emission's characteristics have to be polarization dependent.^{4,5,7} The TM polarization state has an electric field component that is parallel to the grating vector [see inset in Fig. 1(a) for TE and TM definitions].

We introduce a theoretical and experimental investigation of space-variant polarization-dependent thermal emission by exploiting the polarization dependence of the SPPs. Computer-generated subwavelength gratings etched on fused silica (SiO₂) substrates are used to generate space-variant polarization radiation. As a first step, we designed a grating to enhance the nondirectional thermal emission to form a narrow spectral peak for TM polarization. We were then able to experimentally demonstrate space-variant polarization manipulation of thermal emission by discretely controlling the local orientation of the grating. This phenomenon can be exploited in a variety of applications such as thermal polarization imaging, optical encryption, spatially modulated heat transfer, and the formation of high-efficiency thermal sources.⁸

SPPs are supported by polar materials in the spectral range where $\epsilon' < -1$ (ϵ' is the real part of the dielectric constant). There are two kinds of materials that support surface waves: conductive materials that support surface plasmon-polaritons,^{9,10} and dielectric materials that support SPPs. As can be seen in Fig. 1(b), fused silica behaves as a polar material in the spectral range of 8.65 to 9.18 μm .¹¹ Our goal was to design a grating on a SiO₂ substrate for which nondirectional emission was restricted to a narrow spectral band. In opaque materials the emissivity (ϵ) is related to the reflectance (R) via Kirchhoff's law, $\epsilon = 1 - R$ for each direction, wavelength, temperature, and polarization. In

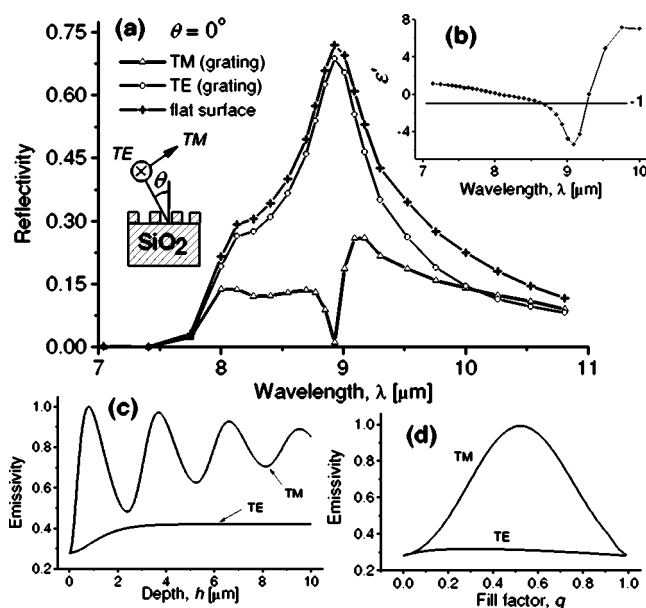


FIG. 1. (a) The calculated SiO₂ spectral reflectance in the normal direction for a flat surface (crosses), and for a grating with period $\Lambda=2 \mu\text{m}$, fill factor $q=0.5$, and depth $h=0.7 \mu\text{m}$ for TM polarization (triangles) and TE polarization (circles). The inset illustrates the illumination scheme of the grating. (b) The spectral dependence of the real part of the SiO₂ dielectric constant, ϵ' . (c) The calculated emissivity vs grating depth for TM and TE polarizations for a wavelength of 8.93 μm in the normal direction of light, with grating parameters: period $\Lambda=2 \mu\text{m}$ and fill factor $q=0.5$. (d) The calculated emissivity vs grating fill factor (q) for TM and TE polarizations for a wavelength of 8.93 μm in the normal direction of light, with grating parameters of: period $\Lambda=2 \mu\text{m}$, depth= $0.7 \mu\text{m}$.

^{a)}Electronic mail: mehasman@tx.technion.ac.il

order to maximize the emissivity, we optimized the SiO₂ grating using a spectral reflectance calculation by rigorous coupled-wave analysis. Figure 1(c) shows the calculation of the emissivity as a function of the grating depth for normal incident light with a wavelength of 8.93 μm. There is a strong variation in the emissivity as a function of the grating depth only for TM polarization.¹² The dependence of the emissivity as a function of the grating's fill factor (q) was also calculated with the previous parameters, but with a grating depth of 0.7 μm as shown in Fig. 1(d). The optimal grating parameters were determined to be: period $\Lambda=2$ μm, fill factor $q=0.5$, and grating depth $h=0.7$ μm.

Figure 1(a) shows the calculated spectral reflectance of the grating for TE and TM polarization states as well as that of the flat surface for normal incident light. Note that for $\lambda=8.93$ μm, the TE reflection coincides with the reflectance of the flat surface, while the TM reflection is close to zero. We ascribe the spectral resonance of the reflectance to the excitation of SPPs. According to Kirchhoff's law, we expected to obtain a high discrimination between the emissivity of the TE and TM polarizations. As a next step, we defined the emissivity modulation to be $\eta=|(\epsilon_{TM}-\epsilon_{TE})/(\epsilon_{TM}+\epsilon_{TE})|$, where ϵ_{TM} and ϵ_{TE} are the emissivity values for the TM and TE polarization states, respectively. The optimized grating parameters cited earlier yielded a high-emissivity modulation of $\eta=0.52$ for angles up to 30°.

In order to confirm our theoretical predictions, we formed a 10 mm × 10 mm uniform grating on an amorphous SiO₂ substrate using advanced photolithographic techniques. A Cr film was deposited on a SiO₂ substrate and overcoated with a positive photoresist. After exposing the photoresist through a mask, it was developed leaving a strip pattern on the Cr film. A Cr etchant was then applied to remove the Cr film from the exposed areas. At this point the photoresist was removed and the substrate etched by reactive ion etching (RIE) through the Cr strips, which served as a mask. The RIE was performed at a power of 175 W and a pressure of 40 mTorr with CF₄ and O₂ gas flow rates of 13.8 and 1.2 sccm, respectively. The etching, performed at a rate of 35 Å/min at room temperature, was continued until the desired depth was reached. As a final step, the remaining Cr was removed with a Cr etchant.

The inset in Fig. 2(b) shows a scanning electron microscope (SEM) image of the grating. Due to inaccuracies in fabrication, the actual fill factor was 0.3 instead of 0.5. For this fill factor the optimal depth was determined to be 0.8 μm instead of 0.7 μm. We began by illuminating the grating with an infrared source (SiC 1270 K, SP-Oriel 80007) at an incidence angle of 20°. We measured the reflectance for both polarization states with an infrared Fourier transform spectrometer (FTIR, SP-Oriel MIR 8000, resolution 4 cm⁻¹) equipped with a cooled HgCdTe detector (SP-Oriel 80026). Figure 2 shows the measured and the calculated spectral reflectance values at 20° incidence to a flat surface and to the grating. The results are in good agreement with the calculated values for both polarizations. For these grating parameters we obtained an emissivity modulation of $\eta=0.33$.

Spectral measurements of the emissivity were then performed by use of FTIR. In this experiment, the sample was heated to 873 K with a precision better than 1 K (heater and temperature controller from HeatWave Labs Inc.). Figure 3 shows the measured and calculated spectral dependence of

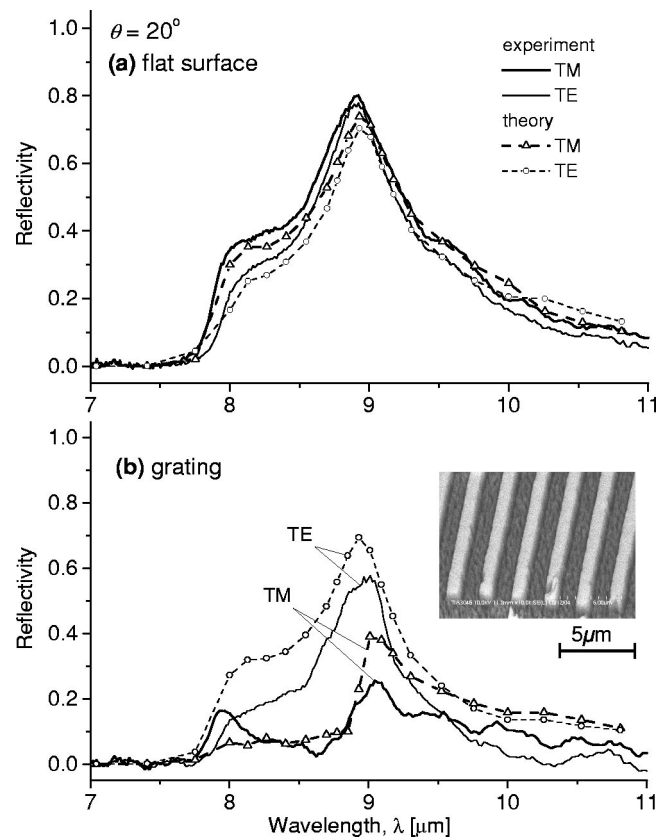


FIG. 2. Measured and calculated spectral reflectance with an incidence angle of $\theta=20^\circ$ of a (a) flat surface and (b) uniform SiO₂ grating. Grating parameters: $\Lambda=2$ μm, fill factor $q=0.3$, and depth $h=0.8$ μm. Experimental results for TE and TM (solid lines), calculated results for TE (dashed line with circles), and for TM polarization (dashed line with triangles). The inset shows SEM image of the grating.

the relative emissivity for TM and TE polarizations, as well as without a polarizer, in a normal emission direction and for $\theta=30^\circ$. The relative emissivity is defined as the grating emissivity (ϵ_G) normalized to the emissivity of the flat surface (ϵ_F) for each case. A narrow spectral peak of $\Delta\lambda=90$ nm was obtained for TM polarization around a wavelength of 9.07 μm. Its relative emissivity was 2.75, while the relative emissivity of TE polarization was approximately unity. The measured peak wavelength of the relative emissivity was shifted with respect to the predicted value. This results from temperature-related variations in the dielectric constant.² The inset in Fig. 3(a) shows both experimental and calculated relative emissivity as a function of the emission angle, and indicates that the peak emissivity was nondirectional. Coupling of the emission in any direction is possible if the SPP dispersion relation is flat.²

Finally, in order to demonstrate space-variant polarization-dependent thermal emission, we formed four space-variant spiral elements having a discrete local groove orientation of $\phi=m\omega/2$, where m is the polarization order and ω is the azimuthal angle of the polar coordinates.^{8,13,14} The elements were 10 mm in diameter with 16 discrete levels and designed for polarization order numbers of $m=1, 2, 3$ and 4. SEM images of the central area of the elements are shown in Fig. 4(a). Figure 4(b) shows the spatial thermal emission distributions after emerging from the spiral elements at 353 K, then passed through a linear polarizer and captured by a thermal camera (CEDIP, 320 × 240 pixels).

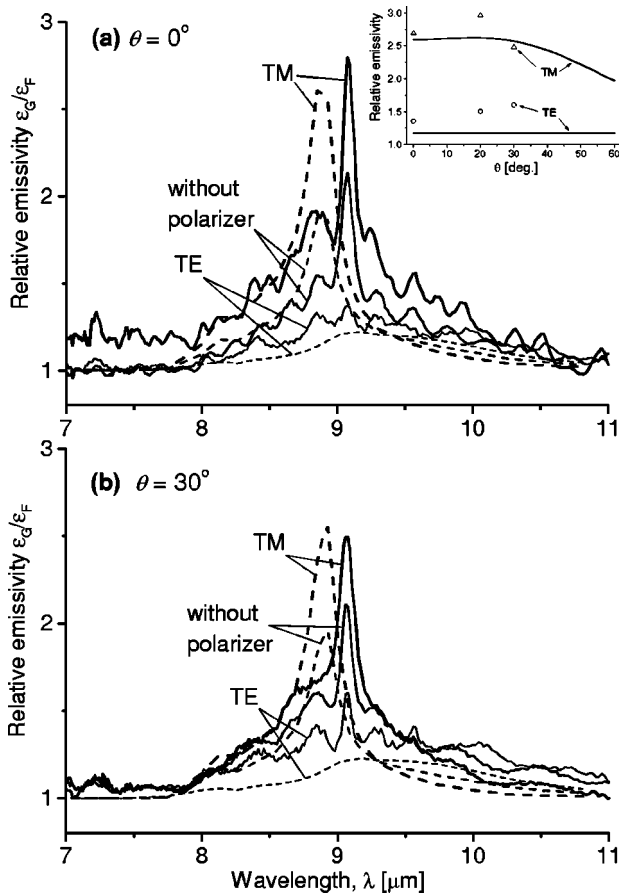


FIG. 3. Measured (solid) and calculated (dashed) relative emissivity spectrum of the grating for TM, TE, and total (without a polarizer) emission in (a) normal observation direction $\theta=0^\circ$ and (b) $\theta=30^\circ$. Inset shows the measured and calculated (solid lines) relative emissivity as a function of observation angle for TM (triangle) and TE (circle) polarization.

Space-variant spiral-like intensity modulation, resulting from the space-variant polarization-dependent emissivity, is clearly observed. The distribution of the emissions from the spiral elements not passed through a polarizer are shown in Fig. 4(c), in which the black lines indicate the local TM polarization orientation. In this case, the emission distribution is almost uniform. However, an axially symmetric polarization orientation is obtained in the near-field for the enhanced TM emission. As expected from Fig. 3, the total intensity emitted from the grating is higher than from the flat surface emission due to the enhanced TM emission.

In conclusion, we have demonstrated a narrow spectral relative emissivity peak for a broad range of observations for a SiO_2 grating. The enhanced thermal infrared radiation,

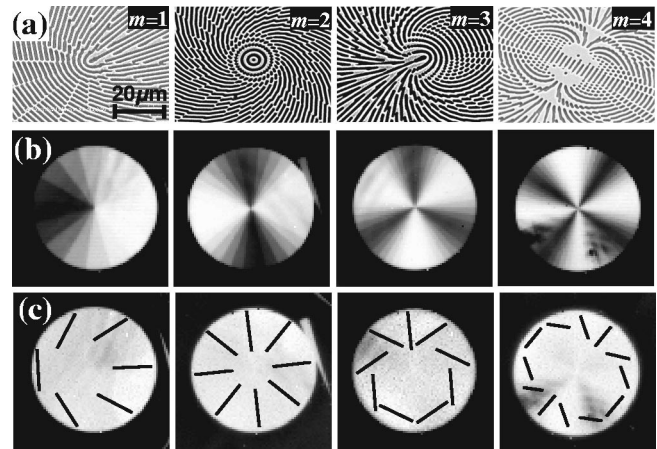


FIG. 4. (a) SEM image of the spiral subwavelength elements with polarization order numbers $m=1, 2, 3,$ and 4 . Thermal emission images emerging from the SiO_2 spiral elements (b) captured through a polarizer and (c) without a polarizer, for $m=1, 2, 3, 4$. The elements were uniformly heated to a temperature of 353 K. The lines indicate the local TM polarization orientation measured in the near-field.

which was obtained only with TM polarization, was attributed to the excitation of SPPs. Using the polarization dependence of the emissivity, a space-variant polarization manipulation of the thermal emission was experimentally demonstrated by controlling the local orientation of the sub-wavelength grating.

- ¹J.-J. Greffet, R. Carminati, K. Joulain, J.-P. Mulet, S. Mainguy, and Y. Chen, *Nature (London)* **416**, 61 (2002).
- ²F. Marquier, K. Joulain, J.-P. Mulet, R. Carminati, J.-J. Greffet, and Y. Chen, *Phys. Rev. B* **69**, 155412 (2004).
- ³P. J. Hesketh, J. N. Zemel, and B. Gebhart, *Nature (London)* **324**, 549 (1986).
- ⁴P. J. Hesketh, J. N. Zemel, and B. Gebhart, *Phys. Rev. B* **37**, 10795 (1988).
- ⁵P. J. Hesketh, J. N. Zemel, and B. Gebhart, *Phys. Rev. B* **37**, 10803 (1988).
- ⁶E. Wolf, *Nature (London)* **326**, 363 (1987).
- ⁷T. Setälä, M. Kaivola, and A. T. Friberg, *Phys. Rev. Lett.* **88**, 123902-1 (2002).
- ⁸E. Hasman, G. Biener, A. Niv, and V. Kleiner, *Progress in Optics*, edited by E. Wolf (Elsevier, Amsterdam, in press), Vol. 47.
- ⁹H. Raether, *Surface Plasmons on Smooth and Rough Surfaces and on Gratings* (Springer, Berlin, 1988).
- ¹⁰W. L. Barnes, A. Dereux, and T. W. Ebbesen, *Nature (London)* **424**, 824 (2003).
- ¹¹E. D. Palik, *Handbook of Optical Constants of Solids* (Academic, New York, 1985).
- ¹²F. Marquier, K. Joulain, and J.-J. Greffet, *Opt. Lett.* **29**, 2178 (2004).
- ¹³A. Niv, G. Biener, V. Kleiner, and E. Hasman, *Opt. Lett.* **29**, 238 (2004).
- ¹⁴A. Niv, G. Biener, V. Kleiner, and E. Hasman, *Opt. Lett.* **28**, 510 (2003).